Numerical simulation of seismic wave propagation in attenuative transversely isotropic media

Ali Fathalian, Daniel O. Trad and Kristopher A. Innanen

ABSTRACT

Simulation of wave propagation in a TTI viscoacoustic medium is an important problem. We have developed a derivation of a system of equations for viscoacoustic waves in a medium with transverse isotropy (TI) in velocity and attenuation based on a standard linear solid model. The resulting system of equations is first order in time for the stress-strain relationship. The numerical implementation of this system determines with the finite-difference method, with second-order accuracy in time and fourth-order accuracy in space. Our results show that the proposed approach for modeling is able of capturing TI effects in attenuation and illustrating the efficiency of this system of equations for applications in seismic imaging and inversion.

INTRODUCTION

Attenuation and anisotropy are increasingly indispensable components of wavefield simulation in seismic exploration and monitoring applications. They are especially important in modern seismic amplitude modeling and reverse time migration (RTM) procedures. The approximate use of the isotropic acoustic approximation in situations involving significant anisotropy and attenuation leads to resolution degradation and mispositioning of reflectors within images (Zhou et al., 2006). In these cases, including anisotropy and viscosity in our physical models is essential; however, the computational expense involved in the use of full elastodynamic equations (i.e., those needed for a proper treatment of anisotropy and viscoelasticity) motivates approximate wave formulations which remain as close as possible to the acoustic case. Alkhalifah (1998, 2000) derived a pseudo-acoustic wave equation from the elastic dispersion relation by setting to zero the shear-wave velocity along the anisotropy symmetry axis. This approach is demanding on memory because of the need to approximate fourth-order partial derivatives of the wavefield. To further reduce the computational cost, the pseudo-acoustic equation was shown to be separable into two coupled second-order partial differential equations using an auxiliary wavefield (Zhou et al., 2006; Du et al., 2008). Transverse isotropic media with a vertical symmetry axis (VTI) are appropriate for thin and approximately horizontal layering or fracturing (Crampin, 1984). Tilted transverse isotropy (TTI) is derived from VTI equations by assuming the symmetry axis is non-vertical and locally variable (Fletcher et al., 2008; Zhang and Zhang, 2008); this formulation is suitable for aligned fractures with a symmetry axis lying between vertical and horizontal. Zero-valued S_V wave velocities on the symmetry axis within the pseudo-acoustic approximation lead to instabilities in the TTI equations associated with the appearance of a residual shear wave (Grechka et al., 2004; Du et al., 2008; Zhang et al., 2009). It is well known that imposing the elliptical anisotropy approximation, i.e., a small smoothly tapered circular region with $\varepsilon = \delta$ around the source, can be effective

in suppressing shear wave artifacts (Du et al., 2008; Zhang and Zhang, 2008; Yoon et al., 2010).
In this work, we derive the equations for a viscoacoustic TI medium with anisotropy in velocity and attenuation based on the standard linear solid model. When the quality factor goes to infinity, the equations reduce to the derived system of equations introduced by Duveneck and Bakker (2011) for TI anisotropic velocity. This paper is organized as follows. First, we introduce our formulation of the approximate viscoacoustic wave equation with transverse isotropy (TI) in velocity and attenuation. Then, we discuss the stability of the computations for a discretization with the finite difference method. Numerical results on 2D synthetic data are presented in the last section.

VISCOACOUSTIC WAVE EQUATION IN TTI MEDIA

In the 2D case, the first-order differential acoustic wave equations of VTI media is expressed as follows (Du et al., 2008):

$$\partial_t \sigma_H = \rho V_P^2 \left[(1+2\varepsilon)\dot{\varepsilon}_{11} + \sqrt{1+2\delta}\dot{\varepsilon}_{33} \right], \tag{1}$$

$$\partial_t \sigma_V = \rho V_P^2 \left[\sqrt{1+2\delta}\dot{\varepsilon}_{11} + \dot{\varepsilon}_{33} \right], \tag{2}$$

where σ_H and σ_V represent the horizontal and vertical stress components respectively. ε and δ are the Thomsen parameters, and the ε_{ij} are the diagonal elements of strain tensor. To obtain the viscoacoustic wave equation in an anisotropic medium, we can modify the acoustic anisotropic medium. In this work, we will focus on anisotropic velocity and isotropic Q, therefore Q is independent of direction. The general stress-strain relationship in viscoelastic media reads (Christensen, 1982)

$$\sigma_{ij} = G_{ijkl} * \dot{\varepsilon}_{kl}, \tag{3}$$

where $*$ denotes convolution in time, σ_{ij} is the stress tensor, ε_{kl} is the strain tensor and G_{ijkl} is the stiffness tensor that determines the behavior of material. We will consider standard linear solid models (SLS) in anelastic anisotropic media. The time response for this model is given by (Blanch et al., 1993)

$$G_{ijkl}(t) = M^R_{ijkl} \left(1 - \frac{1}{L} \sum_{\ell=1}^{L} (1 - \frac{\tau_{\varepsilon\ell}}{\tau_{\sigma\ell}}) e^{-\frac{t}{\tau_{\sigma\ell}}} \right) H(t), \tag{4}$$

where L is the number of mechanism, M^R_{ijkl} is the relaxation modulus of medium (Pipkin, 1986), and $H(t)$ is the heaviside function. The $G_{ijkl}(t)$ is equivalent to a series of L standard linear solid (Blanch et al., 1993), and is also the best Padé approximation for constant-Q (Day and Minster, 1984). Elements $\tau_{\sigma\ell}$ and $\tau_{\varepsilon\ell}$ refer to the stress and strain relaxation times of the ℓth mechanisms. In Voigt notation (using the identification $G_{IJ} \leftrightarrow G_{ijkl}$ by

mapping of indexes $1, 2, 3, 4, 5, 6$ into the pairs $(1,1), (2,2), (3,3), (2,3), (1,3), (1,2)$) the components of the tensor of anelasticity become

$$G_{IJ}(t) = M_{IJ}^R \left(1 - \frac{1}{L}\sum_{\ell=1}^{L}(1 - \frac{\tau_{\varepsilon\ell}}{\tau_{\sigma\ell}})e^{-\frac{t}{\tau_{\sigma\ell}}}\right) H(t), \tag{5}$$

The anelasticity matrix for transversely isotropic media with vertical axis (VTI media) can be written as (Du et al., 2008; da Silva et al., 2019)

$$G_{IJ}(t) = \begin{pmatrix} G_{11} & G_{11}-2G_{66} & G_{13} & 0 & 0 & 0 \\ G_{11}-2G_{66} & G_{11} & G_{13} & 0 & 0 & 0 \\ G_{13} & G_{13} & G_{33} & 0 & 0 & 0 \\ 0 & 0 & 0 & G_{44} & 0 & 0 \\ 0 & 0 & 0 & 0 & G_{44} & 0 \\ 0 & 0 & 0 & 0 & 0 & G_{66} \end{pmatrix}. \tag{6}$$

The elements of the anelasticity tensor can be calculated by definition of the relaxation modulus in VTI media. The relaxation modulus in VTI media can be described in terms of the vertical P- and S- velocities and the Thomsen parameters (Thomsen, 1986). The elements M_{IJ}^R of elastic tensor are related to these quantities by

$$\begin{gathered} M_{11}^R = \rho V_P^2(1+2\varepsilon), \qquad M_{33}^R = \rho V_P^2, \qquad M_{44}^R = \rho V_S^2, \qquad M_{66}^R = \rho V_S^2(1+2\gamma), \\ (M_{13}^R + M_{44}^R)^2 = \rho^2(V_P^2 - V_S^2)^2 + 2\delta\rho^2 V_P^2(V_P^2 - V_S^2). \end{gathered} \tag{7}$$

Applying the acoustic TI approximation, i.e., setting $V_S = 0$, simplifies the elements M_{IJ}^R for VTI media as

$$\begin{gathered} M_{11}^R = \rho V_P^2(1+2\varepsilon), \qquad M_{33}^R = \rho V_P^2, \qquad M_{44}^R = 0, \qquad M_{66}^R = 0, \\ M_{13}^R = \rho V_P^2\sqrt{1+2\delta}. \end{gathered} \tag{8}$$

After the elimination of the shear components, the number of stiffness relaxation parameters is reduced to three components. In viscoacoustic medium with transverse isotropy (TI) in attenuation, the strain relation times dependent on the direction. Hence, we can introduce the strain relaxation time components (horizontal, normal, and vertical) as

$$\begin{gathered} \tau_h^{\varepsilon l} = \tau_{11}^{\varepsilon l}, \tau_n^{\varepsilon l} = \tau_{13}^{\varepsilon l}, \\ \tau_v^{\varepsilon l} = \tau_{33}^{\varepsilon l}. \end{gathered} \tag{9}$$

Eliminating the shear components and substituting expressions 6-9 into equation 5, yields

$$G(t) = \begin{pmatrix} M_{11} & M_{11} & M_{13} \\ M_{11} & M_{11} & M_{13} \\ M13 & M_{13} & M_{33} \end{pmatrix} \left(1 - \frac{1}{L} \sum_{\ell=1}^{L} (1 - \frac{\tau_m^{\varepsilon\ell}}{\tau^{\sigma\ell}}) e^{-\frac{t}{\tau^{\sigma\ell}}} \right) H(t); m = h, n, v. \quad (10)$$

The viscoacoustic wave equation in VTI media can be obtained by a combination of equations 3 and 10. Hence, the relation between stress and strain is given by

$$\begin{aligned} \sigma_H = M_{11}^R \left(1 - \frac{1}{L} \sum_{\ell=1}^{L} (1 - \frac{\tau_h^{\varepsilon\ell}}{\tau^{\sigma\ell}}) e^{-\frac{t}{\tau_{\sigma\ell}}} \right) H(t) * (\dot{\varepsilon}_{11} + \dot{\varepsilon}_{22}) \\ + M_{13}^R \left(1 - \frac{1}{L} \sum_{\ell=1}^{L} (1 - \frac{\tau_n^{\varepsilon\ell}}{\tau^{\sigma\ell}}) e^{-\frac{t}{\tau_{\sigma\ell}}} \right) H(t) * \dot{\varepsilon}_{33}, \end{aligned} \quad (11)$$

$$\begin{aligned} \sigma_V = M_{13}^R \left(1 - \frac{1}{L} \sum_{\ell=1}^{L} (1 - \frac{\tau_n^{\varepsilon\ell}}{\tau^{\sigma\ell}}) e^{-\frac{t}{\tau_{\sigma\ell}}} \right) H(t) * (\dot{\varepsilon}_{11} + \dot{\varepsilon}_{22}) \\ + M_{33}^R \left(1 - \frac{1}{L} \sum_{\ell=1}^{L} (1 - \frac{\tau_v^{\varepsilon\ell}}{\tau^{\sigma\ell}}) e^{-\frac{t}{\tau_{\sigma\ell}}} \right) H(t) * \dot{\varepsilon}_{33}, \end{aligned} \quad (12)$$

where $\sigma_H = \sigma_{11} = \sigma_{22}$ is the horizontal stress component and $\sigma_V = \sigma_{33}$ is the vertical stress component. For the 2D case, taking the time derivative of equations 11 and 12 and using $\partial_t \varepsilon_{ij} = \partial_{xi} u_i$ leads to

$$\begin{aligned} \partial_t \sigma_H = & M_{11}^R \left(1 - \frac{1}{L} \sum_{\ell=1}^{L} (1 - \frac{\tau_h^{\varepsilon\ell}}{\tau^{\sigma\ell}}) \right) \partial_x u_x \\ & + M_{11}^R \left(1 - \frac{1}{L} \sum_{\ell=1}^{L} \frac{1}{\tau^{\sigma\ell}} (1 - \frac{\tau_h^{\varepsilon\ell}}{\tau^{\sigma\ell}}) e^{-\frac{t}{\tau^{\sigma\ell}}} \right) H(t) * \partial_x u_x \\ & + M_{13}^R \left(1 - \frac{1}{L} \sum_{\ell=1}^{L} (1 - \frac{\tau_n^{\varepsilon\ell}}{\tau^{\sigma\ell}}) \right) \partial_z u_z \\ & + M_{13}^R \left(1 - \frac{1}{L} \sum_{\ell=1}^{L} \frac{1}{\tau^{\sigma\ell}} (1 - \frac{\tau_n^{\varepsilon\ell}}{\tau^{\sigma\ell}}) e^{-\frac{t}{\tau^{\sigma\ell}}} \right) H(t) * \partial_z u_z, \end{aligned} \quad (13)$$

$$\begin{aligned}\partial_t \sigma_V =& M_{13}^R \left(1 - \frac{1}{L}\sum_{\ell=1}^{L}(1 - \frac{\tau_n^{\varepsilon\ell}}{\tau^{\sigma\ell}}\right) \partial_x u_x \\ &+ M_{13}^R \left(1 - \frac{1}{L}\sum_{\ell=1}^{L}\frac{1}{\tau^{\sigma\ell}}(1 - \frac{\tau_n^{\varepsilon\ell}}{\tau^{\sigma\ell}})e^{-\frac{t}{\tau^{\sigma\ell}}}\right) H(t) * \partial_x u_x \\ &+ M_{33}^R \left(1 - \frac{1}{L}\sum_{\ell=1}^{L}(1 - \frac{\tau_v^{\varepsilon\ell}}{\tau^{\sigma\ell}}\right) \partial_z u_z \\ &+ M_{33}^R \left(1 - \frac{1}{L}\sum_{\ell=1}^{L}\frac{1}{\tau^{\sigma\ell}}(1 - \frac{\tau_v^{\varepsilon\ell}}{\tau^{\sigma\ell}})e^{-\frac{t}{\tau^{\sigma\ell}}}\right) H(t) * \partial_z u_z,\end{aligned} \tag{14}$$

where u_x, and u_z are components of the particle velocity vector. The convolution term in these equations can be eliminated by introducing memory variables (Carcione et al., 1988). Hence, equations 13 and 14 reduce to

$$\begin{aligned}\partial_t \sigma_H = M_{11}^R \left(1 - \frac{1}{L}\sum_{\ell=1}^{L}(1 - \frac{\tau_h^{\varepsilon\ell}}{\tau_{\sigma\ell}}\right) \partial_x u_x + M_{13}^R \left(1 - \frac{1}{L}\sum_{\ell=1}^{L}(1 - \frac{\tau_n^{\varepsilon\ell}}{\tau_{\sigma\ell}}\right) \partial_z u_z \\ + \frac{1}{L}\sum_{\ell=1}^{L}(M_{11}^R r_H + M_{13}^R r_N),\end{aligned} \tag{15}$$

$$\begin{aligned}\partial_t \sigma_V = M_{13}^R \left(1 - \frac{1}{L}\sum_{\ell=1}^{L}(1 - \frac{\tau_n^{\varepsilon\ell}}{\tau_{\sigma\ell}}\right) \partial_x u_x + M_{33}^R \left(1 - \frac{1}{L}\sum_{\ell=1}^{L}(1 - \frac{\tau_v^{\varepsilon\ell}}{\tau_{\sigma\ell}}\right) \partial_z u_z \\ + \frac{1}{L}\sum_{\ell=1}^{L}(M_{13}^R r_N + M_{33}^R r_V),\end{aligned} \tag{16}$$

where $r_{H\ell}$, $r_{N\ell}$, and $r_{V\ell}$, are memory variables of horizontal, normal and vertical stress components

$$r_{H\ell} = \left(\frac{1}{\tau^{\sigma\ell}}(1 - \frac{\tau_h^{\varepsilon\ell}}{\tau^{\sigma\ell}})e^{-\frac{t}{\tau^{\sigma\ell}}}\right) H(t) * \partial_x u_x, \tag{17}$$

$$r_{N\ell} = \left(\frac{1}{\tau^{\sigma\ell}}(1 - \frac{\tau_n^{\varepsilon\ell}}{\tau^{\sigma\ell}})e^{-\frac{t}{\tau^{\sigma\ell}}}\right) H(t) * \partial_{x,z} u_{x,z}, \tag{18}$$

$$r_{V\ell} = \left(\frac{1}{\tau^{\sigma\ell}}(1-\frac{\tau_v^{\varepsilon\ell}}{\tau^{\sigma\ell}})e^{-\frac{t}{\tau^{\sigma\ell}}}\right) H(t) * \partial_z u_z, 1 \leq \ell \leq L. \tag{19}$$

A set of first-order linear differential equations for the memory variables can be obtained by taking the time derivative of equations 17-19. We obtain

$$\begin{aligned}\dot{r}_{H\ell} = &-\frac{1}{\tau^{\sigma\ell}}\left(\frac{1}{\tau^{\sigma\ell}}(1-\frac{\tau_h^{\varepsilon\ell}}{\tau^{\sigma\ell}})e^{-\frac{t}{\tau^{\sigma\ell}}}\right) H(t) * \partial_x u_x \\ &+\left(\frac{1}{\tau^{\sigma\ell}}(1-\frac{\tau_h^{\varepsilon\ell}}{\tau^{\sigma\ell}})e^{-\frac{t}{\tau^{\sigma\ell}}}\right) \delta(t) * \partial_x u_x,\end{aligned} \tag{20}$$

$$\begin{aligned}\dot{r}_{N\ell} = &-\frac{1}{\tau^{\sigma\ell}}\left(\frac{1}{\tau^{\sigma\ell}}(1-\frac{\tau_n^{\varepsilon\ell}}{\tau^{\sigma\ell}})e^{-\frac{t}{\tau^{\sigma\ell}}}\right) H(t) * \partial_{x,z} u_{x,z} \\ &+\left(\frac{1}{\tau^{\sigma\ell}}(1-\frac{\tau_n^{\varepsilon\ell}}{\tau^{\sigma\ell}})e^{-\frac{t}{\tau^{\sigma\ell}}}\right) \delta(t) * \partial_{x,z} u_{x,z},\end{aligned} \tag{21}$$

$$\begin{aligned}\dot{r}_{V\ell} = &-\frac{1}{\tau^{\sigma\ell}}\left(\frac{1}{\tau^{\sigma\ell}}(1-\frac{\tau_v^{\varepsilon\ell}}{\tau^{\sigma\ell}})e^{-\frac{t}{\tau^{\sigma\ell}}}\right) H(t) * \partial_z u_z \\ &+\left(\frac{1}{\tau^{\sigma\ell}}(1-\frac{\tau_v^{\varepsilon\ell}}{\tau^{\sigma\ell}})e^{-\frac{t}{\tau^{\sigma\ell}}}\right) \delta(t) * \partial_z u_z,\end{aligned} \tag{22}$$

Substituting equations 17-19 into equation 20-22, gives

$$\dot{r}_{H\ell} = -\frac{1}{\tau^{\sigma\ell}} r_{H\ell} + \left(\frac{1}{\tau^{\sigma\ell}}(1-\frac{\tau_h^{\varepsilon\ell}}{\tau^{\sigma\ell}})\right) \partial_x u_x, \tag{23}$$

$$\dot{r}_{N\ell} = -\frac{1}{\tau^{\sigma\ell}} r_{N\ell} + \left(\frac{1}{\tau^{\sigma\ell}}(1-\frac{\tau_n^{\varepsilon\ell}}{\tau^{\sigma\ell}})\right) \partial_{x,z} u_{x,z}, \tag{24}$$

$$\dot{r}_{V\ell} = -\frac{1}{\tau^{\sigma\ell}} r_{V\ell} + \left(\frac{1}{\tau^{\sigma\ell}}(1-\frac{\tau_v^{\varepsilon\ell}}{\tau^{\sigma\ell}})\right) \partial_z u_z. \tag{25}$$

A combination of the equations of motion and the stress-strain relationships leads to a system of first-order differential equations that describe the wave propagation in the viscoacoustic medium. Hence, the viscoacoustic wave equation in anisotropic media for a series of SLS can be written as

$$\partial_t u_x = (1/\rho)\partial_x \sigma_H, \tag{26}$$

$$\partial_t u_z = (1/\rho)\partial_z \sigma_V, \tag{27}$$

$$\begin{aligned}\partial_t \sigma_H =& \rho V_P^2 \left[(1+2\varepsilon) \left(\left[1 - \sum_{\ell=1}^{L} \left(1 - \frac{\tau_h^{\varepsilon\ell}}{\tau^{\sigma\ell}} \right) \right] \partial_x u_x + \frac{1}{L} \sum_{\ell=1}^{L} r_{H\ell} \right) \right] \\ &+ \rho V_P^2 \sqrt{1+2\delta} \left[\left(1 - \sum_{\ell=1}^{L} \left(1 - \frac{\tau_n^{\varepsilon\ell}}{\tau^{\sigma\ell}} \right) \right) \partial_z u_z + \frac{1}{L} \sum_{\ell=1}^{L} r_{N\ell} \right],\end{aligned} \tag{28}$$

$$\begin{aligned}\partial_t \sigma_V =& \rho V_P^2 \left[\sqrt{1+2\delta} \left(\left[1 - \sum_{\ell=1}^{L} \left(1 - \frac{\tau_n^{\varepsilon\ell}}{\tau^{\sigma\ell}} \right) \right] \partial_x u_x + \frac{1}{L} \sum_{\ell=1}^{L} r_{N\ell} \right) \right] \\ &+ \rho V_P^2 \left[\left(1 - \sum_{\ell=1}^{L} \left(1 - \frac{\tau_{\varepsilon\ell}}{\tau_{\sigma\ell}} \right) \right) \partial_z u_z + \frac{1}{L} \sum_{\ell=1}^{L} r_{V\ell} \right].\end{aligned} \tag{29}$$

The simplest and most practical approximations for anisotropic media is VTI medium, while only valid for simple geologic formations. In anticline structures and thrust sheets where sediments are steeply dipping, the VTI medium approximation is not useful because of non-vertical symmetry axis of the medium. However, to avoid the image blurring and mispositioning, we must consider the tilted symmetry. One way to calculate the TTI equations is to locally rotate the coordinate system of VTI medium. The rotation matrix as function of the polar angle and azimuth angle is defined as

$$\mathbf{R} = \begin{pmatrix} \cos\theta\cos\varphi & \cos\theta\sin\varphi & -\sin\theta \\ -\sin\varphi & \cos\varphi & 0 \\ \sin\theta\cos\varphi & \sin\theta\sin\varphi & \cos\theta \end{pmatrix}, \tag{30}$$

where θ represent the tilt angle and φ represent the azimuth of tilt for TTI symmetry axis. The spatial derivative in a rotated coordinate system can be written as

$$\begin{pmatrix} \partial_{x'} \\ \partial_{y'} \\ \partial_{z'} \end{pmatrix} = \mathbf{R} \begin{pmatrix} \partial_x \\ \partial_y \\ \partial_z \end{pmatrix}, \tag{31}$$

where primed ($\prime$) refer to the rotated coordinate system. Substituting equation 31 into equations 26 to 29, the 2D viscoacoustic wave equation in anisotropic TTI media for a series of SLS can be written as

$$\partial_t u_x = (1/\rho)\partial_{x'}\sigma_H, \tag{32}$$

$$\partial_t u_z = (1/\rho)\partial_{z'}\sigma_V, \tag{33}$$

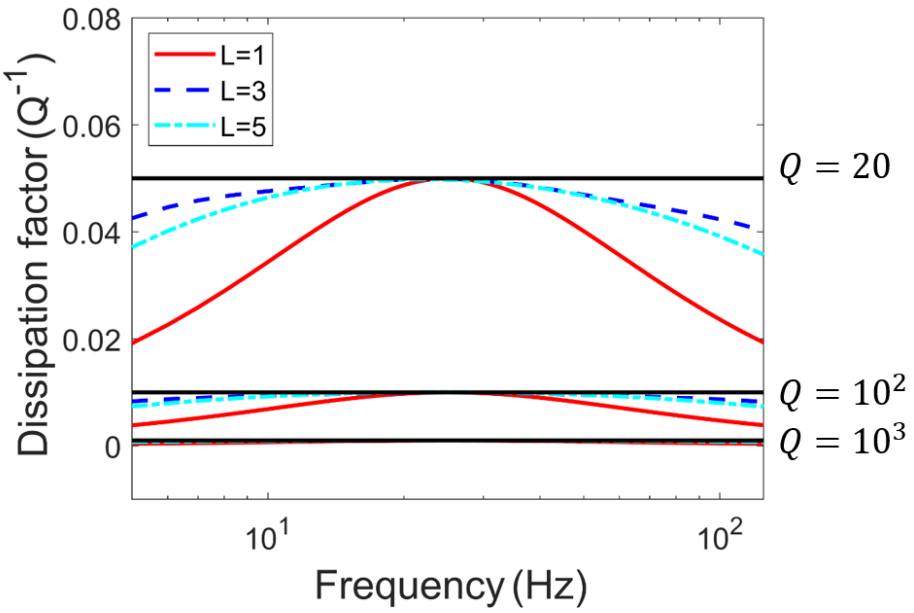

FIG. 1. Comparison of the dissipation factors for different number of mechanisms (L) in the weak and strong attenuating media.

$$\begin{aligned}\partial_t \sigma_H =& \rho V_P^2 \left[(1+2\varepsilon) \left(\left[1 - \sum_{\ell=1}^{L} \left(1 - \frac{\tau_h^{\varepsilon\ell}}{\tau^{\sigma\ell}} \right) \right] \partial_{x'} u_x + \frac{1}{L} \sum_{\ell=1}^{L} r_{H\ell} \right) \right] \\ &+ \rho V_P^2 \sqrt{1+2\delta} \left[\left(1 - \sum_{\ell=1}^{L} \left(1 - \frac{\tau_n^{\varepsilon\ell}}{\tau^{\sigma\ell}} \right) \right) \partial_{z'} u_z + \frac{1}{L} \sum_{\ell=1}^{L} r_{N\ell} \right],\end{aligned} \tag{34}$$

$$\begin{aligned}\partial_t \sigma_V =& \rho V_P^2 \left[\sqrt{1+2\delta} \left(\left[1 - \sum_{\ell=1}^{L} \left(1 - \frac{\tau_n^{\varepsilon\ell}}{\tau^{\sigma\ell}} \right) \right] \partial_{x'} u_x + \frac{1}{L} \sum_{\ell=1}^{L} r_{N\ell} \right) \right] \\ &+ \rho V_P^2 \left[\left(1 - \sum_{\ell=1}^{L} \left(1 - \frac{\tau_{\varepsilon\ell}}{\tau_{\sigma\ell}} \right) \right) \partial_{z'} u_z + \frac{1}{L} \sum_{\ell=1}^{L} r_{V\ell} \right].\end{aligned} \tag{35}$$

where $\partial_{x'}$ and $\partial_{z'}$ are the first order differential operators in the rotated coordinate system aligned with the symmetry axis:

$$\partial_{x'} = \cos\theta \cos\varphi \partial_x - \sin\theta \partial_z, \tag{36}$$

$$\partial_{z'} = \cos\varphi \sin\theta \partial_x + \cos\theta \partial_z. \tag{37}$$

ATTENUATION MODEL IN ANISOTROPIC MEDIA

There is physical evidence that attenuation is almost linear with frequency (therefore Q is constant) in many frequency bands. Constant-Q models provide an efficient parameterization of seismic attenuation in rocks and can improve the seismic inversion by reducing the number of parameters. Kjartansson (1979) used a linear model for attenuation of the wave with Q independent of frequency, without any cut-offs, which is mathematically simple and completely specified by phase velocity and Q. Kjartansson's constant-Q model is mathematically simpler than any model with nearly constant-Q as a spectrum of general standard linear solid (GSLS) models (Carcione, 2007). A simple combination of SLSs requires a relatively large number of solids to obtain a constant quality factor over a wide frequency band. The selection of the number of relaxation mechanisms (L) is quite important since the increase of required computational memory and time is proportional to the used number of relaxation mechanisms.
Blanch et al. (1995) propose the τ-method that is based on the simple observation that the level of attenuation caused by an SLS can be determined by a dimensionless (frequency scale-independent) variable τ as

$$\tau = \frac{\tau^{\varepsilon\iota}}{\tau^{\sigma\iota}} - 1, \tag{38}$$

where $\tau^{\varepsilon\iota}$ and $\tau^{\sigma\iota}$ are the strain and stress relaxation parameters respectively (Robertsson et al., 1994). τ is a function of quality factor (Q), and an optimal value of that is sufficient to control a constant Q response over a frequency band of interest. In order to evaluate the accuracy of a series of single standard linear solid mechanisms, the dissipation factor (Q^{-1}) of one, three and five SLS mechanisms compare with the theoretical model. Figure 1 shows the dissipation factor in weak attenuation media (Q=1000 and Q=100) and the dissipation factor in strong attenuation media (Q=20). The reference velocity is 2.5 km/s, and the frequency band is 5 -125 Hz. in weak attenuation media, the three SLS mechanism fits the theoretical model curves very well in the specified frequency band. Note, the one, three, and five SLS have a good approximation to the phase velocity and dissipation factor around the reference frequency. In strong attenuation media, like the weak attenuation case, we found that the three SLS mechanism fits the theoretical model curves in the particularized frequency band, and the single and five SLS mechanisms have a good approximation to the phase velocity and dissipation factor around the reference frequency. In strong attenuation media, the error of single SLS is more significant than the weak attenuation media, while in the center frequency all SLS mechanisms are fit to the theoretical result.
We can use a similar approach for anisotropic attenuating media. The variable T can be defined as

$$\tau_m = \frac{\tau_m^{\varepsilon\iota}}{\tau_m^{\sigma\iota}} - 1, m = h, n, v. \tag{39}$$

where h, n, and v refer to the horizontal, normal, and vertical components respectively. In anisotropic attenuating media, similar to the isotropic attenuating media approach, the values of τ_m are computed for each Q_m.

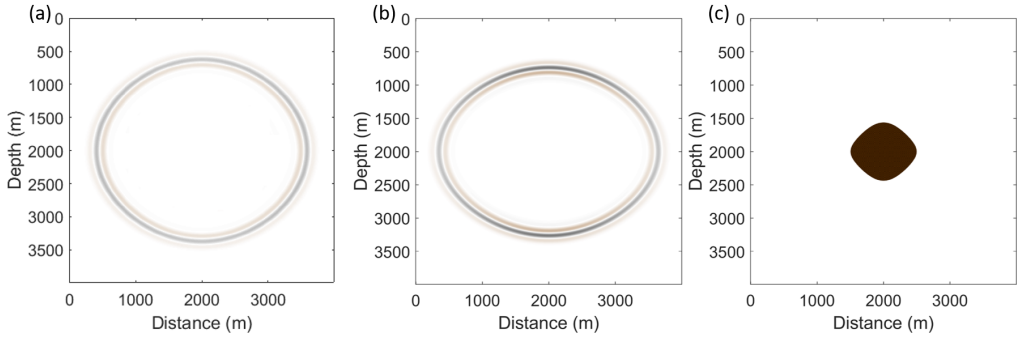

FIG. 2. Illustrate a snapshot of wavefield in VTI media: (a) isotropic attenuation(δt = 1 ms), (b) anisotropic attenuation (δt = 1 ms), and (c) the unstable wavefield at δt = 1.01 ms.

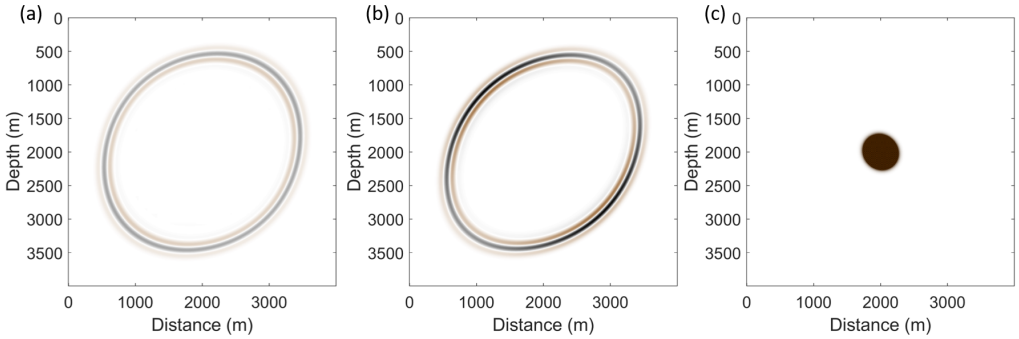

FIG. 3. Illustrate a snapshot of wavefield in TTI media with θ=45° and φ=0°: (a) isotropic attenuation(δt = 1.09 ms), (b) anisotropic attenuation (δt = 1.09 ms), and (c) the unstable wavefield at δt = 1.1 ms.

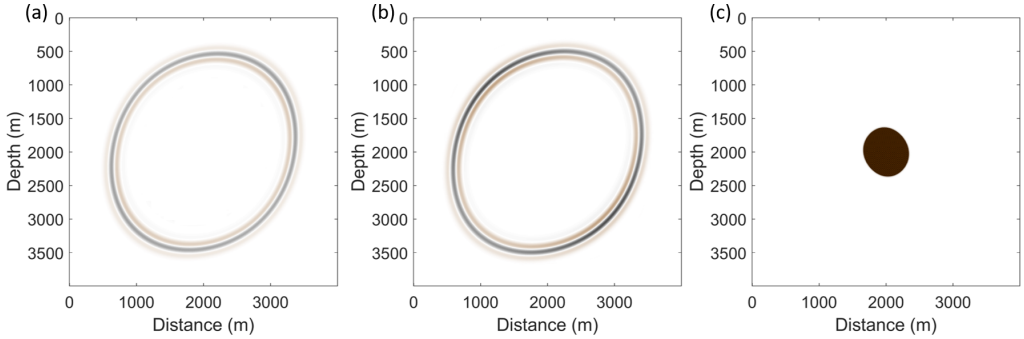

FIG. 4. Illustrate a snapshot of wavefield in TTI media with θ=45° and φ=20°: (a) isotropic attenuation(δt = 1.13 ms), (b) anisotropic attenuation (δt = 1.13 ms), and (c) the unstable wavefield at δt = 1.14 ms.

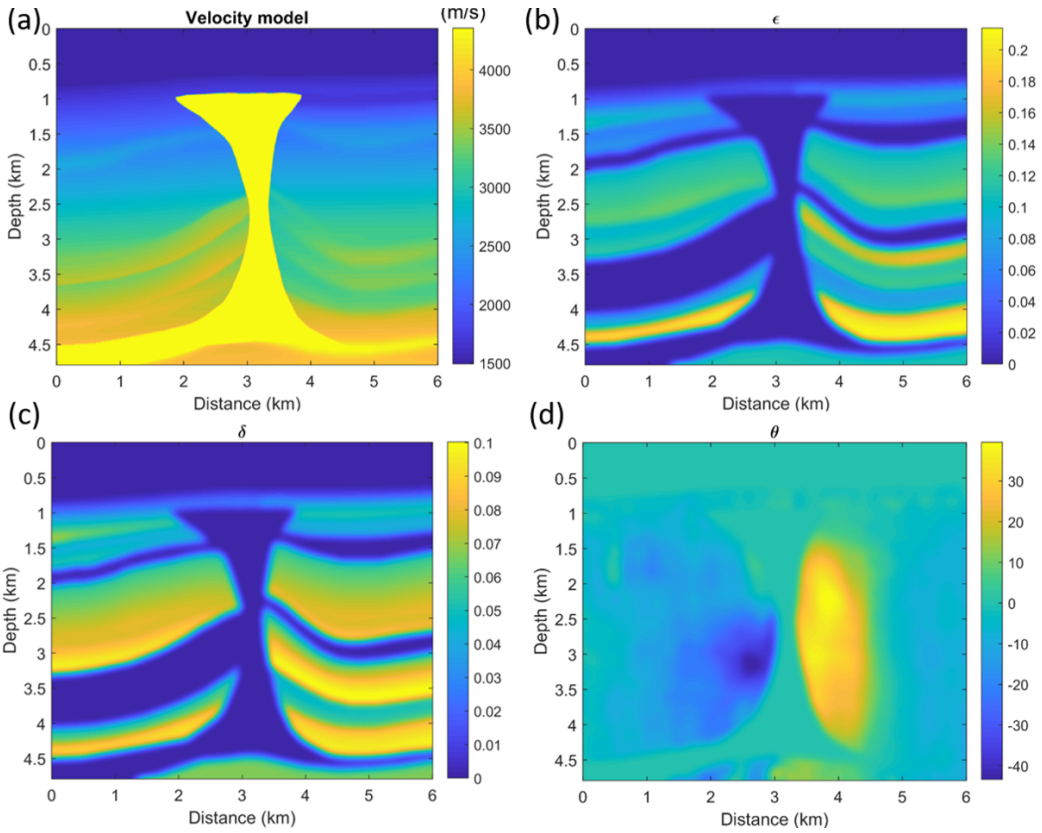

FIG. 5. A portion of BP model: (a) velocity model, (b) Thomsen's ε model, (c) Thomsen's δ model, and (d) tilt angle in degrees.

ANISOTROPIC VISCOACOUSTIC SYNTHETIC MODEL

To verify the anisotropic viscoacoustic wave equations(32-35), showing the dependence of the attenuation with direction, we consider the homogenous model with velocity V= 2000 m/s, ε = 0.2, and δ = 0. We examine the numerical character of the solutions of the wave equation as created using the unsplit-field PML boundary approach (Fathalian et al., 2020). First, we consider a VTI medium (θ=0 and φ=0).

A snapshot of the wavefield computed with a time-step length of 1 ms, using the anisotropic and isotropic models of attenuation, is shown in Figure 2. Our results show that the computation of the wavefield remains stable, and the wavefront is elliptical. In the isotropic attenuation model (Figure 2a), the level of attenuation along the entire wavefront is the same, while in the anisotropic attenuation model (Figure 2b), the amplitude of the wavefront is weaker for energy propagating along the horizontal direction than that propagating along the vertical direction. Figure 2c shows a snapshot of the wavefield with a time step of 1.01 ms. The result indicates that the computation becomes unstable at this time step.

In the second example, we investigate the TTI medium with a tilt angle, $\theta = 45^\circ$ and an azimuth angle, $\varphi = 0^\circ$. In the isotropic attenuation case (Figure 3a), the amplitude is the same along the wavefront. When the model of attenuation is anisotropic, the amplitude of

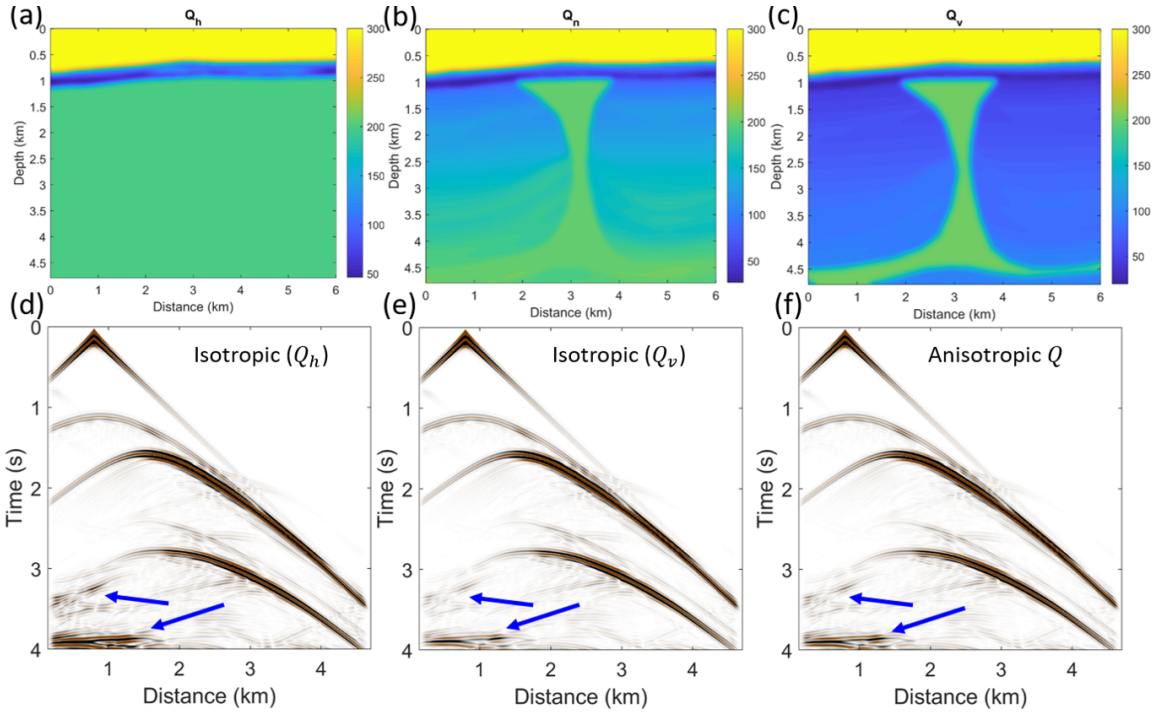

FIG. 6. (a-c) Quality factors of horizontal, vertical, and normal components. Shot gather computed with (c) isotropic attenuation with Q=Q_h, (d) isotropic model of attenuation with Q= Q_v, and (c) anisotropic model of attenuation.

the wavefront is different in different directions. Figure 3c shows the computation of the wavefield with a time step of 1.1 ms is not stable. Finally, we consider the TTI medium with a tilt angle, $\theta = 45^\circ$ and an azimuth angle, $\varphi = 20^\circ$ (Figure 4). Similar to the above results, in anisotropic attenuation media, the attenuation of the wavefield is not the same in different directions (Figure 4b).

ANISOTROPIC VISCOACOUSTIC BP MODEL

To verify our code, we consider the more realistic 2D TTI BP model. Figure 5 presents the velocity, tilt angle, and the associated Thomsen parameter models. The corresponding horizontal, normal, and vertical components of the Q model are shown in Figure 7a, 7b and 7c, respectively. As before, shear-wave artifacts are avoided by setting up small tapered circular regions with $\varepsilon = \delta$ around the source positions (Du et al., 2008). The model grid dimensions are 1176×1501, and the grid size is 4×4 m. Sources and receivers are positioned along the surface at a depth of 30 m, and a zero-phase Ricker wavelet with a 15 Hz center frequency is adopted. Within this model, we generate viscoacoustic synthetic data sets when attenuation is anisotropic and isotropic for a source placed at the leftmost position. We consider three different cases for the model of attenuation including, (1) the isotropic attenuation model (setting Q_v and Q_n equal to Q_h (Figure 7a)), (2) the isotropic attenuation model by setting Q_h and Q_n equal to Q_v (Figure 7b), and (3) the anisotropic attenuation model (Q_h, Q_v, and Q_n components are given by the models illustrated in Figure

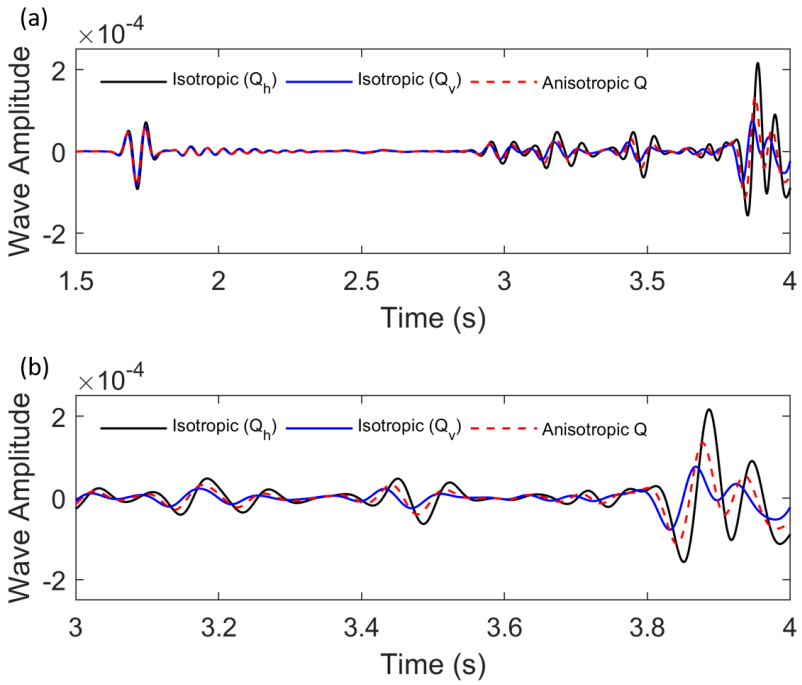

FIG. 7. (a)Comparison of three traces extracted from the snapshot wavefield images in Figure 7. (b) Magnified view of Figure 8a.

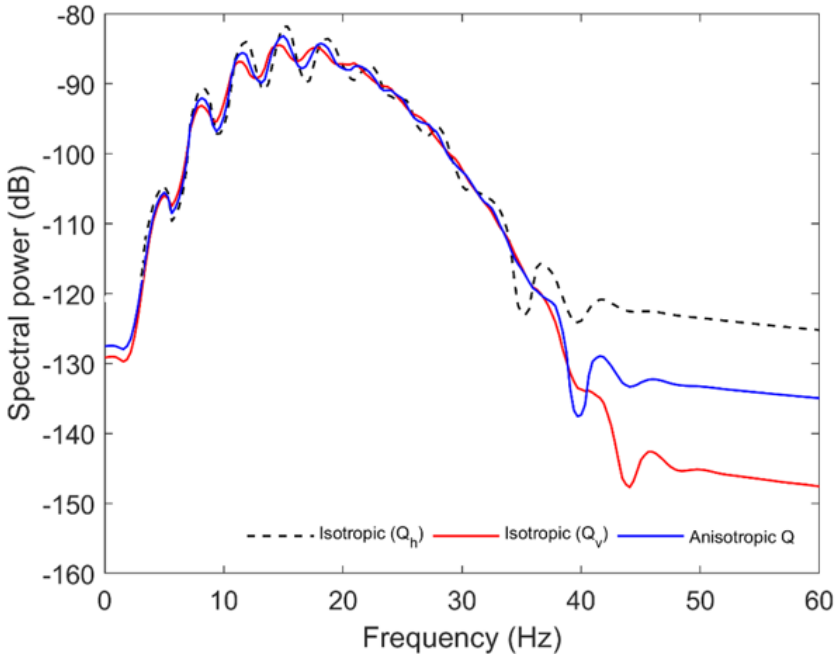

FIG. 8. Comparison of the amplitude spectrum for the traces for each one of the different models of attenuation.

7a-7c, respectively). For these attenuation models, we generate the shot gathers in Figure 7. In the first case (Q=Q_h), the amplitude of the waveform is not attenuated strongly because the attenuation media is weak (Figure 7a). For the second (Figure 7b) and third (Figure 7c) attenuation model, we observe that there are no effects of attenuation in the energy recorded at the shorter offsets, while at longer offsets and larger recording times, the effect of attenuation is visible because the energy has propagated throughout the high attenuating zones. To prove our results, we compare the traces for three models of attenuation. Our results show that there is no significant difference between phases and amplitudes at the short offsets (Figure 8a). However, at the larger offsets, we observe the different phases and amplitudes (Figure 8b). The traces of anisotropic attenuating medium (the dashed red line) show that the phase delay and amplitude are located between the two isotropic attenuation model results. Hence, the data generated by the anisotropic model can not be explained by the isotropic models. Spectra computed from the shot records, plotted in Figure 9, illustrate the effect of attenuation in the amplitude spectrum for each one of the traces in Figure 8. We observe that the amplitude spectra are very similar at the near offset, while at the long offset the spectrum becomes damped by increasing frequency. Also, the result indicates that the amplitude spectrum for the anisotropic attenuating medium locates in between the two isotropic attenuation model results that confirm the result of Figure 8.

CONCLUSIONS

We have presented an approach for modeling viscoacoustic waves with transverse isotropy (TI) in velocity and attenuation. We derived partial differential equations in first-order in time by eliminating the shear components based on the standard linear solid model. Our modeling approach is demonstrating a good accuracy for modeling seismic waves in media with anisotropy and attenuation. Also, this approach is stable in media with a rapid change of tilt angle and strong contrast in the physical properties. The proposed approach is useful for seismic modeling, imaging, and inversion.

ACKNOWLEDGMENTS

We thank the sponsors of CREWES for continued support. This work was funded by CREWES industrial sponsors, NSERC (Natural Science and Engineering Research Council of Canada) through the grants CRDPJ 461179-13 and CRDPJ 543578-19. Partial funding also came from the Canada First Research Excellence Fund.

REFERENCES

Alkhalifah, T., 1998, Acoustic approximations for processing in transversely isotropic media: Geophysics, **63**, No. 2, 623–631.

Alkhalifah, T., 2000, An acoustic wave equation for anisotropic media: Geophysics, **67**, 1304–1325.

Blanch, J. O., Robertsson, J. O., and Symes, W. W., 1993, Viscoelastic finite-difference modeling, *in* Expanded Abstracts, 990–993.

Carcione, J. M., 2007, Wave fields in real media: Wave propagation in anisotropic, anelastic, porous and electromagnetic media: Elsevier.

Carcione, J. M., Kosloff, D., and Kosloff, R., 1988, Wave propagation simulation in a linear viscoacoustic medium: Geophysical Journal International, **93**, No. 2, 393–401.

Christensen, R., 1982, Theory of Viscoelasticity, An Introduction: Academic Press, New York.

Crampin, S., 1984, Anisotropy in exploration seismics: First Break, **2**, 19–21.

da Silva, N. V., Yao, G., and Warner, M., 2019, Wave modeling in viscoacoustic media with transverse isotropy: Geophysics, **84**, No. 1, no. 1, C41–C56.

Day, S. M., and Minster, J. B., 1984, Numerical simulation of attenuated wavefields using a padé approximant method: Geophysical Journal International, **78**, No. 1, 105–118.

Du, X., Fletcher, R. P., and Fowler, P. J., 2008, A new pseudo-acoustic wave equation for VTI medium, *in* Expanded Abstracts, H033.

Duveneck, E., and Bakker, P. M., 2011, Stable P-wave modeling for reverse-time migration in tilted TI media: Geophysics, **76**, No. 2, no. 2, S65–S75.

Fathalian, A., Trad, D. O., and Innanen, K. A., 2020, An approach for attenuation-compensating multidimensional constant-Q viscoacoustic reverse time migration: Geophysics, **85**, No. 1, no. 1, S33–S46.

Fletcher, R., Du, X., and Fowler, P. J., 2008, A new pseudo-acoustic wave equation for TI media, *in* Expanded Abstracts, 2082–2086.

Grechka, V., Zhang, L., and Rector III, J. W., 2004, Shear waves in acoustic anisotropic media: Geophysics, **69**, No. 2, 576–582.

Kjartansson, E., 1979, Constant Q-wave propagation and attenuation: Journal of Geophysical Research: Solid Earth, **84**, No. B9, 4737–4748.

Pipkin, A., 1986, Lectures on Viscoelasticity Theory: Springer.

Robertsson, J. O. A., Blanch, J. O., and Symes, W. W., 1994, Viscoelastic finite-difference modeling: Geophysics: Geophysics, **59**, 1444–1456.

Thomsen, L., 1986, Weak elastic anisotropy: Geophysics, **51**, No. 10, 1954–1966.

Yoon, K., Suh, S., Ji, J., Cai, J., and Wang, B., 2010, Stability and speedup issues in TTI RTM implementation, *in* Expanded Abstracts, 3221–3225.

Zhang, H., Zhang, G., and Zhang, Y., 2009, Removing S-wave noise in TTI reverse time migration, *in* Expanded Abstracts, 2849–2853.

Zhang, H., and Zhang, Y., 2008, Reverse time migration in 3D heterogeneous TTI media, *in* Expanded Abstracts, 2196–2200.

Zhou, H. B., Zhang, G. Q., and Bloor, R., 2006, An anisotropic acoustic wave equation for modeling and migration in 2D TTI medium, *in* Expanded Abstracts, 194–198.